

Spin dynamics of heterometallic Cr₇M wheels (M = Mn, Zn, Ni) probed by inelastic neutron scattering

R. Caciuffo and T. Guidi

*Dipartimento di Fisica ed Ingegneria dei Materiali e del Territorio,
Università Politecnica delle Marche, Via Brecce Bianche, I-60131 Ancona, Italy*

G. Amoretti, S. Carretta, E. Livioti, and P. Santini

Dipartimento di Fisica, Università di Parma, I-43100 Parma, Italy

C. Mondelli

*Istituto Nazionale per la Fisica della Materia, and Institut Laue Langevin,
Boîte Postale 220 X, F-38042 Grenoble Cedex, France*

G. Timco, C. A. Muryn and R.E.P. Winpenny

*Department of Chemistry, The University of Manchester,
Oxford Road, Manchester, M13 9PL, United Kingdom*

Inelastic neutron scattering has been applied to the study of the spin dynamics of Cr-based antiferromagnetic octanuclear rings where a finite total spin of the ground state is obtained by substituting one Cr³⁺ ion ($s = 3/2$) with Zn ($s = 0$), Mn ($s = 5/2$) or Ni ($s = 1$) di-cations. Energy and intensity measurements for several intra-multiplet and inter-multiplet magnetic excitations allow us to determine the spin wavefunctions of the investigated clusters. Effects due to the mixing of different spin multiplets have been considered. Such effects proved to be important to correctly reproduce the energy and intensity of magnetic excitations in the neutron spectra. On the contrary to what is observed for the parent homonuclear Cr₈ ring, the symmetry of the first excited spin states is such that anticrossing conditions with the ground state can be realized in the presence of an external magnetic field. Heterometallic Cr₇M wheels are therefore good candidates for macroscopic observations of quantum effects.

PACS numbers: 75.50.Tt, 75.10.Jm, 75.40.Gb, 75.45.+j

I. INTRODUCTION

Magnetic wheels are polynuclear molecular clusters with a ring-shaped cyclic structure and a dominant antiferromagnetic (AF) coupling between nearest-neighbor ions. For an even number of spin centers, the ground state is a singlet and the excitation spectrum is characterized by rotational and spin-wave like bands [1, 2, 3]. Heterometallic rings with $S \neq 0$ can be obtained from an $S = 0$ homonuclear ring by chemical substitution of one or two magnetic centers [4, 5]. Theoretical calculations suggest that such systems could exhibit interesting quantum-coherence phenomena [6, 7] and are therefore of considerable interest. Indeed, the replacement of a magnetic ion in a cyclic structure allows one to modify the topology of the exchange interactions, that in turn plays a key role in determining the macroscopic behavior of the system [8, 9, 10].

Here we report the results of inelastic neutron scattering (INS) experiments on heterometallic AF rings, and we show that the spin level sequence and dynamics are substantially modified with respect to those of the parent compound. The investigated wheels are derived from the spin-compensated neutral [Cr₈F₈(O₂CCMe₃)₁₆] ring [11] by substitution of one divalent cation (M = Mn, Zn, Ni) for a trivalent Cr ion [4]. Due to the difference between the Cr³⁺ spin ($s = 3/2$) and the spin of the dication, the

ground state of the so-obtained Cr₇M wheels has a non-zero total spin ($S = 1/2, 1$ and $3/2$ for M = Ni, Mn and Zn respectively). Recent investigations have shown that, within this Cr₇M family, $S = 3/2$ rings exhibit magnetocaloric effects that could be exploited below $T \sim 2$ K [12], whilst Cr₇Ni could be a suitable candidate for the physical implementation of qubits [13]. The suggested opportunities are linked to properties that are very sensitive to the spin energy spectrum and to the composition of the spin wavefunctions. A reliable determination of these quantities is therefore relevant, and INS is known to be the most appropriate technique to address this problem [14, 15, 16, 17].

Our INS experiments on Cr₇M provide energy and intensity for several transitions between the anisotropy-split lowest spin multiplets. The analysis of the data leads to an accurate determination of the main features of the microscopic intra-cluster interactions, including nearest-neighbor isotropic exchange, zero-field splitting and dipole-dipole interaction parameters (inter-cluster interactions are very weak, of the order of 10 neV). The results obtained indicate that anticrossing conditions between the ground state and excited low-lying energy levels with the same symmetry can be met in Cr₇M, by applying a suitable magnetic field. This is at variance with the situation in the parent Cr₈ ring, where ground state crossings involve states with different symmetry

[15], as confirmed by the vanishingly small level repulsion observed by heat capacity measurements [18]. The occurrence of anticrossing conditions suggests that Cr_7M wheels are good candidates for the macroscopic observation of quantum phenomena arising from S-mixing, such as the quantum fluctuation of the magnitude of the total spin [8, 9].

A correct interpretation of the experimental spectra requires a generalization of the orientation-averaged INS cross-sections for polycrystals [19], as proposed by Waldmann [20].

II. EXPERIMENTAL DETAILS

Deuterated micro-crystalline samples of $(\text{C}_2\text{D}_5)_2\text{NH}_2$ [$\text{Cr}_7\text{MF}_8(\text{O}_2(\text{C}_5\text{D}_9))_{16}$] ($\text{M}^{2+} = \text{Ni}, \text{Mn}, \text{Zn}$) have been prepared according to a slightly modified literature procedure [4, 5], by dissolving chromium fluoride tetrahydrate (Aldrich) in a mixture of trimethyl- d_9 -acetic acid and diethyl- d_{10} -amine (98% deuterated, Aldrich) before adding an excess of the second metal salt (nickel carbonate hydroxide tetrahydrate, manganese chloride tetrahydrate or basic zinc carbonate). The preparation of trimethyl- d_9 -acetic acid starting from acetone- d_6 was adapted from standard methods [21]. All compounds were purified additionally on a silica gel column using toluene as the eluent [4] and finally crystallized from a mixture of pentane/acetone by evaporation of the mixture of solvents at 313-318 K. X-ray diffraction analyses for all three compounds showed that crystals don't have any solvent molecules in the crystal lattice. The observed Bragg peaks could be indexed in the tetragonal $P4$ space group, with lattice parameters at 100 K of $a = b = 19.9598(2)$ Å, $c = 16.0609(2)$ Å for Cr_7Ni ; $a = b = 19.9375(2)$ Å, $c = 16.1079(2)$ Å for Cr_7Mn and $a = b = 19.8973(2)$ Å, $c = 16.0227(2)$ Å for Cr_7Zn . The magnetic rings have a diameter of about 10 Å and the metal ions have the shape of an almost regular planar octagon (Figure 1).

INS measurements have been performed at the Institute Laue-Langevin in Grenoble (France), with the direct-geometry time-of-flight spectrometer IN5, using about 2 grams of each compound. A flat disk geometry has been chosen for the aluminum sample holder (1.1 mm thickness, 5 cm diameter), in order to reduce multiple-scattering background. Neutron spectra have been recorded with the sample kept at different temperatures, between $T = 2$ K and $T = 12$ K, inside a standard liquid- ^4He cryostat. Solid angle and detector efficiency calibrations have been performed using the spectrum of a vanadium metal sample. Neutron incident wavelengths $\lambda = 4$ Å, 5 Å and 9 Å were used, corresponding to instrumental resolutions at the elastic peak of 0.147 meV, 0.091 meV, and 0.019 meV respectively. The three sets of measurements allowed us to cover an energy-transfer range from $\hbar\omega \sim 0.04$ meV to about 4 meV. The angular interval spanned by the detector banks corresponds to

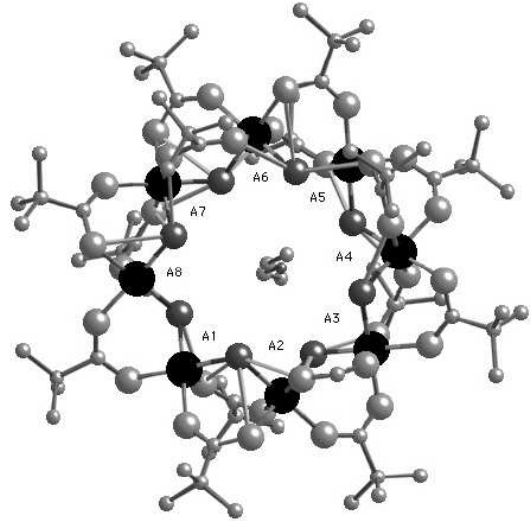


FIG. 1: The molecular structure of the Cr_7M ($\text{M} = \text{Mn}, \text{Ni}, \text{Zn}$) magnetic ring, with hydrogen atoms omitted for clarity. The A ions ($A = 7/8$ Cr and $1/8$ M at each site) are represented by large dark circles; fluorine positions are indicated by small dark circles, the oxygen and carbon atoms are large and small gray circles, respectively. The cation is found H-bonded inside the cavity.

scattering vector amplitudes varying between $Q \sim 0.55$ Å $^{-1}$ and 2.6 Å $^{-1}$ at $\hbar\omega \sim 1$ meV, and between $Q \sim 0.85$ Å $^{-1}$ and 2.2 Å $^{-1}$ at $\hbar\omega \sim 3.7$ meV (for $\lambda = 4$ Å).

III. SPIN HAMILTONIAN AND INS MAGNETIC CROSS SECTION

The investigated systems are ensembles of independent identical magnetic units, each one described by the Hamiltonian operator:

$$H = \sum_{i=1}^6 J_{Cr-Cr} \mathbf{s}_i \cdot \mathbf{s}_{i+1} + J_{Cr-M} (\mathbf{s}_7 \cdot \mathbf{s}_8 + \mathbf{s}_8 \cdot \mathbf{s}_1) + \sum_{i=1}^8 \mathbf{s}_i \cdot \mathbf{D}_i \cdot \mathbf{s}_i + \sum_{i < j=1}^8 \mathbf{s}_i \cdot \mathbf{D}_{ij} \cdot \mathbf{s}_j. \quad (1)$$

In the above equation we assume that sites $i = 1 - 7$ of the octanuclear ring are occupied by Cr^{3+} ions, and site $i = 8$ is filled by the M dication. The first term is the isotropic, nearest-neighbor Heisenberg-Dirac-Van Vleck exchange interaction, with J_{Cr-Cr} and J_{Cr-M} being the exchange integrals for Cr-Cr and Cr-M pairs, respectively. The second term in Eq. 1 describes the local crystal-field interaction, whereas the third term gives the dipole-dipole intra-cluster interaction, evaluated within the point-dipole approximation. Assuming the $\hat{\mathbf{z}}$ -axis along the perpendicular to the ring plane, the second-order local anisotropy is expected to be dominated by the axial terms d_i , with smaller rhombic terms e_i :

$$\sum_{i=1}^8 \mathbf{s}_i \cdot \mathbf{D}_i \cdot \mathbf{s}_i = \sum_{i=1}^8 d_i [s_{z,i}^2 - \frac{1}{3}s_i(s_i+1)] + \sum_{i=1}^8 e_i [s_{x,i}^2 - s_{y,i}^2]. \quad (2)$$

With $s_i \leq 3/2$, no fourth-order local anisotropy must be considered.

As pointed out by Waldmann [20], the INS cross-section described in [19] for polycrystalline samples of molecular nanomagnets is not of general validity. In particular, it may fail to describe correctly the scattering from systems with large magnetic anisotropy and does not properly take into account intramolecular interfer-

ence effects. Here we use the following expression, which is obtained by averaging the magnetic dipole INS cross-section [22] with respect to the possible orientations of the scattering vector \mathbf{Q} [20]:

$$\frac{\partial^2 \sigma}{\partial \Omega \partial \omega} = \frac{A}{N_m} \frac{k_f}{k_0} e^{-2W} \sum_{n,m} \frac{e^{-\beta E_n}}{Z} I_{nm}(Q) \delta(\hbar\omega - E_m + E_n), \quad (3)$$

where $A = 0.29$ barn, N_m is the number of magnetic ions, Z is the partition function, \mathbf{k}_f and \mathbf{k}_0 are the wavevectors of the scattered and incident neutrons, $\exp(-2W)$ is the Debye-Waller factor, $\mathbf{Q} = \mathbf{k}_0 - \mathbf{k}_f$ is the scattering vector, E_n is the energy of the generic spin state $|n\rangle$, and the function $I_{nm}(Q)$ is defined as:

$$I_{nm}(Q) = \sum_{i,j} F_i^*(Q) F_j(Q) \times \left\{ \frac{2}{3} [j_0(QR_{ij}) + C_0^2 j_2(QR_{ij})] \tilde{s}_{z_i} \tilde{s}_{z_j} + \frac{2}{3} [j_0(QR_{ij}) - \frac{1}{2} C_0^2 j_2(QR_{ij})] (\tilde{s}_{x_i} \tilde{s}_{x_j} + \tilde{s}_{y_i} \tilde{s}_{y_j}) + \frac{1}{2} j_2(QR_{ij}) [C_2^2 (\tilde{s}_{x_i} \tilde{s}_{x_j} - \tilde{s}_{y_i} \tilde{s}_{y_j}) + C_{-2}^2 (\tilde{s}_{x_i} \tilde{s}_{y_j} + \tilde{s}_{y_i} \tilde{s}_{x_j})] + j_2(QR_{ij}) [C_1^2 (\tilde{s}_{z_i} \tilde{s}_{x_j} + \tilde{s}_{x_i} \tilde{s}_{z_j}) + C_{-1}^2 (\tilde{s}_{z_i} \tilde{s}_{y_j} + \tilde{s}_{y_i} \tilde{s}_{z_j})] \right\}, \quad (4)$$

where $F(Q)$ is the magnetic form factor, \mathbf{R}_{ij} gives the relative position of ions i and j ,

$$\begin{aligned} C_0^2 &= \frac{1}{2} [3(\frac{R_{ijz}}{R_{ij}})^2 - 1] \\ C_2^2 &= \frac{R_{ijx}^2 - R_{ijy}^2}{R_{ij}^2} \\ C_{-2}^2 &= 2 \frac{R_{ijx} R_{ijy}}{R_{ij}^2} \\ C_1^2 &= \frac{R_{ijx} R_{ijz}}{R_{ij}^2} \\ C_{-1}^2 &= \frac{R_{ijy} R_{ijz}}{R_{ij}^2}, \end{aligned} \quad (5)$$

and

$$\tilde{s}_{\alpha_i} \tilde{s}_{\gamma_j} = \langle n | s_{\alpha_i} | m \rangle \langle m | s_{\gamma_j} | n \rangle \quad (\alpha, \gamma = x, y, z). \quad (6)$$

Eq. 4 is the explicit form of the formula given by Waldmann in [20]. Besides being valid whatever the symmetry and amplitude of the magnetic anisotropy, Eq. 4 can be easily implemented in a numeric code.

The parameters of the spin Hamiltonian (Eqs. 1-2) have been determined from a best fit of the neutron spectra based on calculations of Eq. 4. We recall that from the INS selection rules only transitions with $\Delta S = 0, \pm 1$

and $\Delta M = 0, \pm 1$ have non-zero intensity. In the fitting procedure, a Gaussian lineshape is associated with each allowed transition, with a Full Width at Half Maximum (FWHM) equal to the instrumental resolution and an area proportional to the calculated transition strength. For high-energy transitions, a broadening of the final state reflecting lifetimes effects has been assumed. The parameters defining the Hamiltonian have then been varied until the best agreement between calculated and experimental spectra was obtained.

The anisotropic part of the spin Hamiltonian can be written in terms of irreducible tensor operators (ITO) of rank $k = 2$, and therefore mixes states with different S and M , or at least states with different S if the anisotropy is purely axial. Therefore the total spin S is not a good quantum number and the total Hamiltonian cannot be diagonalized within each $(2S+1)$ -dimensional block. This difficulty can be overcome by the procedure proposed in [23] and used to evaluate the mixing between the lowest lying S multiplets in the Cr_8 ring [15].

First, the minimum ensemble of spin manifolds required to reproduce the INS cross-section at high-energy transfer is determined assuming isotropic exchange only. Then the complete Hamiltonian is diagonalized in the corresponding subspace. In this way one obtains the energy spectrum and the spin states $|n\rangle$ as linear combinations of basis vectors $|(\tilde{S})SM\rangle$ labelled by the set of intermediate spin states (\tilde{S}) , with coefficients $\langle(\tilde{S})SM|n\rangle$.

A stringent test for the spectroscopic assignment of

the observed transitions is provided by the Q dependence of their intensity, which is essentially determined by the geometry of the cluster and the composition of the spin wavefunctions. This dependence can be easily measured with properly calibrated detectors at different scattering angles, and the results can be compared with calculations using Eq. 4.

IV. EXPERIMENTAL RESULTS

A. Cr_7Ni

Figure 2 shows the angle-integrated INS intensity recorded at $T = 2$ K for the Cr_7Ni sample, with IN5 operated at $\lambda = 5$ Å. The two peaks emerging at 1.19 meV and 1.34 meV correspond to transitions between the $|S = 1/2, M = \pm 1/2\rangle$ ground state and the anisotropy split sublevels of the $|S = 3/2\rangle$ first excited spin state, $|S = 3/2, M = \pm 1/2\rangle$ and $|S = 3/2, M = \pm 3/2\rangle$. The solid line represents the intensity corresponding to

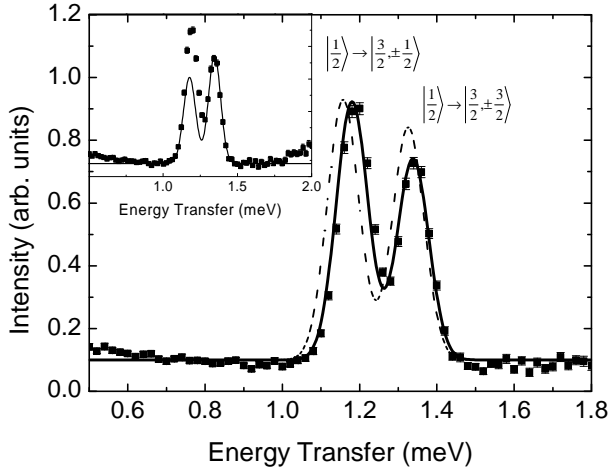


FIG. 2: Low energy transfer INS response for Cr_7Ni at 2 K ($\lambda = 5$ Å). The displayed intensity is the sum for the whole detector bank. Background from the sample holder has been subtracted. Solid line: intensity calculated for the model Hamiltonian described in the text, taking into account S-mixing; broken line: calculated response with S-mixing set to zero. Inset: intensity calculated with the approximate formula for the cross-section given in ref.[19] (solid line).

the Hamiltonian given by Eqs. (1-2), with parameters $J_{\text{Cr}-\text{Cr}} = 1.46$ meV, $J_{\text{Cr}-\text{Ni}} = 1.69$ meV, $d_{\text{Cr}} = -0.03$ meV, and $d_{\text{Ni}} = -0.6$ meV. The d_{Cr} value is the one determined for the Cr_8 ring [15] and was kept fixed in the fitting procedure. As the INS response appears to be quite insensitive to the in-plane anisotropy, the non-axial part of the Hamiltonian has been neglected. With the parameters determined in this work, the ground state composition is dominated by the $|S = 1/2\rangle$ component, with a small $|S = 3/2\rangle$ contamination (about 1%); the first excited state is an almost pure $|S = 3/2\rangle$ multi-

plet with easy-plane zero-field splitting. The INS cross-section has been calculated using the expression given by Eq. 4, integrated over the Q interval corresponding to the experimental conditions. Although quantitatively small, S-mixing must be taken into account to reproduce correctly the intensity ratio of the observed doublet (the intensity calculated with S-mixing neglected is shown in Figure 2 by the dashed line).

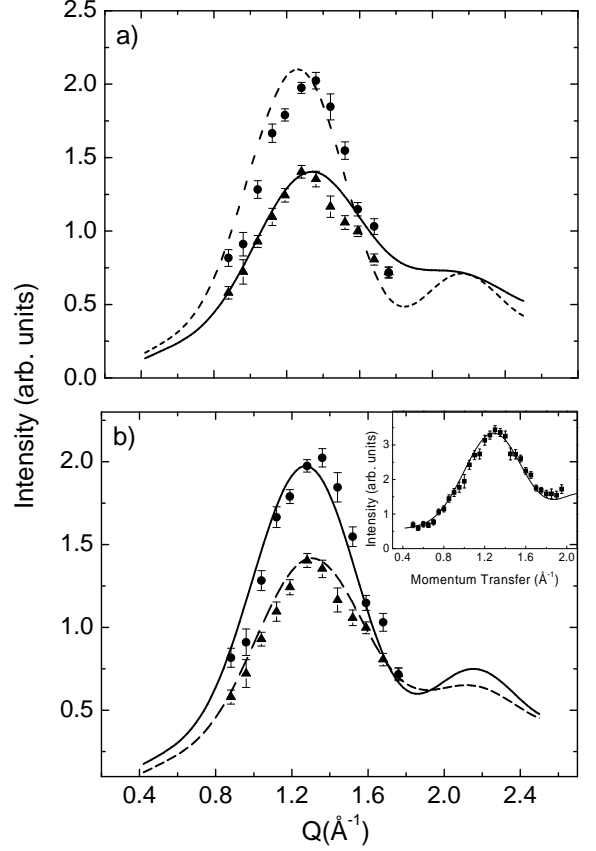


FIG. 3: Cr_7Ni INS intensity of the peaks at 1.19 meV (circles) and 1.34 meV (triangles) as a function of the scattering vector amplitude, Q . Data have been obtained with incident wavelength $\lambda = 5$ Å and sample temperature $T = 2$ K. Calculated curves are represented by solid lines (to be compared with filled circles) and dashed lines (to be compared with triangles). Panel a) shows the result obtained with the INS cross-section as reported in [19], panel b) shows the output of Eq. 4. In both cases $J_{\text{Cr}-\text{Cr}} = 1.46$ meV, $J_{\text{Cr}-\text{Ni}} = 1.69$ meV, $d_{\text{Cr}} = -0.03$ meV, and $d_{\text{Ni}} = -0.6$ meV. The inset in panel b) shows the INS response integrated from 1.1 and 1.4 meV as a function of Q , compared with the calculated curve.

In the inset of Figure 2, the experimental data are compared with the curve calculated by the approximate INS cross-section reported in ref. [19], and the Hamiltonian parameters quoted above. Due to the large anisotropy at the Ni site, the Borrás-Almenar et al. approximation is not adequate in the present case, and its use instead of Eq. 4 would lead to a completely wrong estimate of the Hamiltonian parameters. This difference is more evident

when comparing the Q dependence of the transition intensities with theoretical estimates provided by the two formulae. As shown in Figure 3a, the intensity of the transition involving the $|S = 3/2, M = \pm 1/2\rangle$ excited level at 1.19 meV is underestimated over a large Q interval by the expression given in [19], whilst the intensity of the transition towards the $|S = 3/2, M = \pm 3/2\rangle$ state at 1.34 meV is overestimated by more than a factor two. In comparison, an excellent agreement between calculated curves and observed data is obtained when using Eq. 4 (Figure 3b).

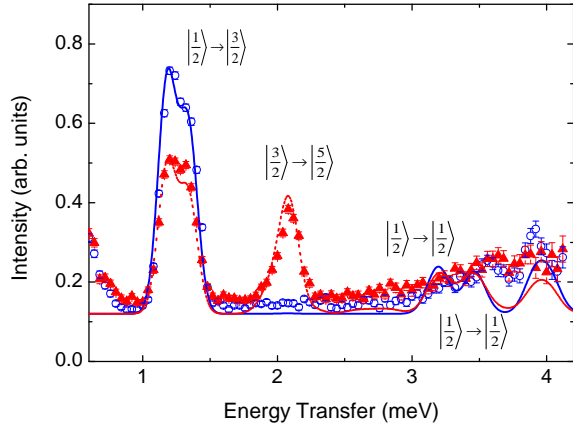


FIG. 4: Cr_7Ni INS spectra collected with $\lambda = 4 \text{ \AA}$ at $T = 2 \text{ K}$ (circles) and $T = 12 \text{ K}$ (triangles). Smooth lines represent the spectra calculated from eigenvalues and eigenvectors of the Hamiltonian given in Eqs.1-2, by associating to each transition a Gaussian lineshape with a height proportional to the calculated probability and a width of $147 \mu\text{eV}$, corresponding to the experimental resolution.

Excitations involving spin manifolds with higher energy can be observed by reducing the incident wavelength. Results obtained with $\lambda = 4 \text{ \AA}$ at $T = 2 \text{ K}$ and $T = 12 \text{ K}$ are shown in Figure 4. At $T = 2 \text{ K}$, weak excitations are observed between 3 and 4 meV. They correspond to transitions from the ground state to $|S = 1/2\rangle$ and $|S = 3/2\rangle$ excited states. When the sample is warmed at 12 K, a strong peak appears at 2.08 meV. This excitation is attributed to the transition from the first excited $|S = 3/2\rangle$ state to a $|S = 5/2\rangle$ state lying at 3.31 meV. The calculated spectra, represented by the smooth lines in Figure 4, compare very favorably with the experiment and confirm the validity of the proposed set of parameters. The ratio $J_{\text{Cr-Ni}}/J_{\text{Cr-Cr}} = 1.16$ is somewhat larger than the recent estimate based on the fit of heat capacity and torque magnetometry data [13]. In addition the weighted average axial anisotropy parameter $d = -0.045 \text{ meV}$ [24] is about 1.7 times larger than previously reported, because of the very large anisotropy of the Ni ion that was not estimated in previous works.

B. Cr_7Zn

Substitution of a diamagnetic Zn^{2+} ion for one Cr^{3+} in the AF Cr_8 ring results in a $|S = 3/2\rangle$ spin ground state, whose anisotropy splitting can be observed by high-resolution INS experiments. Figure 5 shows the spectra recorded on IN5 with incident wavelength 9 \AA (energy resolution at the elastic peak of $19 \mu\text{eV}$), with the sample kept at 2 and 10 K.

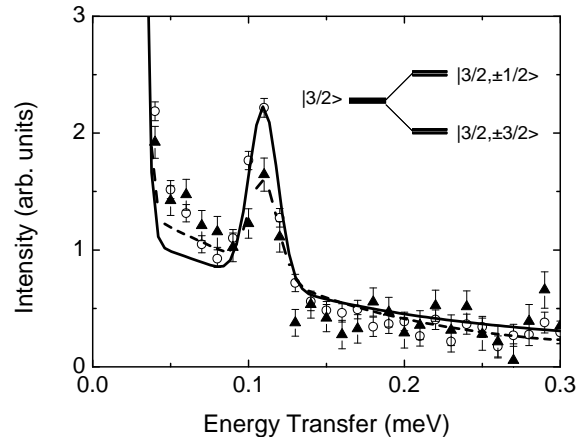


FIG. 5: Cr_7Zn high-resolution INS spectra collected with $\lambda = 9 \text{ \AA}$ at $T = 2 \text{ K}$ (circles) and $T = 10 \text{ K}$ (triangles). The peak at 0.11 meV is an intra-multiplet transition involving the anisotropy split components of the $|S = 3/2\rangle$ ground state. Solid (2 K) and dashed (10 K) lines are intensities calculated for a purely axial, easy plane magnetic anisotropy of the Cr ions ($d_{\text{Cr}} = -0.028 \text{ meV}$). The elastic peak and a quasielastic contribution have been included in the best fit procedure.

Assuming crystal-field parameters similar to those determined in the Cr_8 parent compound, we expect an easy-axis anisotropy for the $S = 3/2$ ground manifold and an easy-plane splitting for the lowest $S = 5/2$ multiplet. In this hypothesis, the peak observed at about 0.11 meV must be attributed to the $|S = 3/2, M = \pm 3/2\rangle \rightarrow |S = 3/2, M = \pm 1/2\rangle$ transition, as only the lowest manifold is thermally populated at $T = 2 \text{ K}$. The solid and broken lines give the calculated intensity for $T = 2$ and 10 K assuming a purely axial local crystal field for the Cr ions, with $d_{\text{Cr}} = -0.028 \text{ meV}$ ($d_{\text{Zn}} = 0$). As for the Ni case, the INS spectra are not sensitive to the in-plane component of the anisotropy and again we consider only the axial part of H .

As shown in Figure 6, intermultiplet transitions at higher energy transfer are observed with incident wavelengths of 4 and 5 \AA . The peaks appearing in the $T = 2 \text{ K}$ spectrum are due to transitions from the split $|S = 3/2\rangle$ ground state towards $|S = 1/2\rangle$ (0.83 meV), $|S = 5/2\rangle$ (1.91 meV), $|S = 1/2\rangle$ and $|S = 3/2\rangle$ (2.25 meV), $|S = 1/2\rangle$ (3.0 meV), and unresolved $|S = 5/2\rangle$ and $|S = 3/2\rangle$ states (3.6 meV).

The spurious peak at 0.4 meV in panel b is due to neutrons diffused incoherently by the sample and diffracted

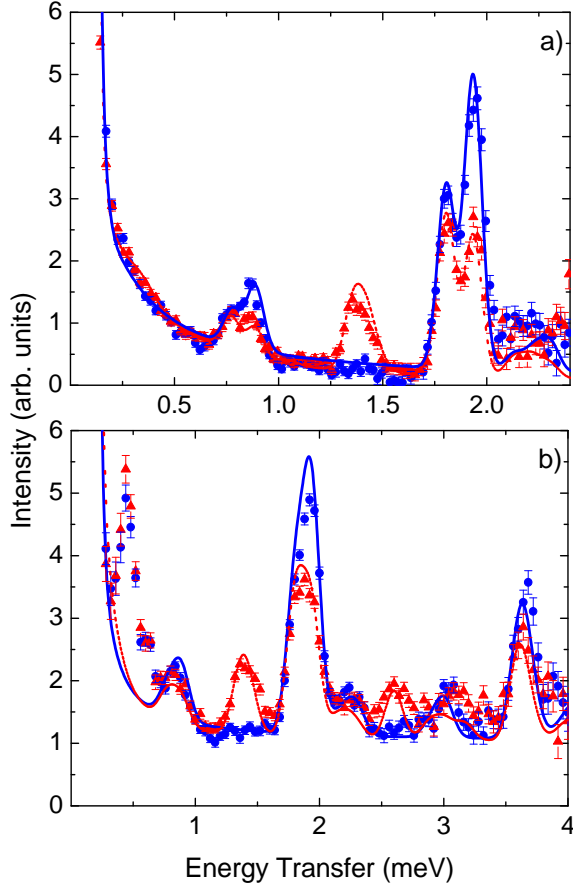


FIG. 6: INS spectra for Cr_7Zn at 2 K (circles) and 12 K (triangles), measured with incident wavelength of (a) 5 Å and (b) 4 Å. The 0.4 meV peak in panel b is spurious. Smooth lines are best fits of the experimental data to a superposition of Gaussian line-shapes associated to allowed transitions. Each Gaussian contribution has an area proportional to the transition strength calculated with Eq. 4 assuming isotropic exchange ($J_{\text{Cr-Cr}} = 1.43$ meV, $J_{\text{Cr-Zn}} = 0$) and axial local anisotropy ($d_{\text{Cr}} = -0.028$ meV).

by the cryostat walls. The instrumental resolution in this configurations is not high enough to resolve the small anisotropy splitting of the excited levels, so that the energy separation of the doublets around 0.83 and 1.91 meV reflects the splitting of the ground state. Hot peaks associated to excitations from the first excited $|S = 1/2\rangle$ level appear at $T = 12$ K around 1.39 and 2.6 meV. The solid and broken lines in Figure 6 are intensities calculated at the two temperatures assuming an exchange parameter very similar to the one reported for the Cr_8 ring in ref. [15], $J_{\text{Cr-Cr}} = 1.43$ meV for every nearest-neighbor Cr-Cr pairs, $J_{\text{Cr-Zn}} = 0$ (as Zn is diamagnetic) and $d_{\text{Cr}} = -0.028$ meV. The agreement with experimental data is very good and justifies the use of just one value for the $J_{\text{Cr-Cr}}$ exchange integrals, although the use of a less symmetric magnetic model would improve the fitting at high energy transfer. The spectroscopic assignments are confirmed by the Q dependence of the transition in-

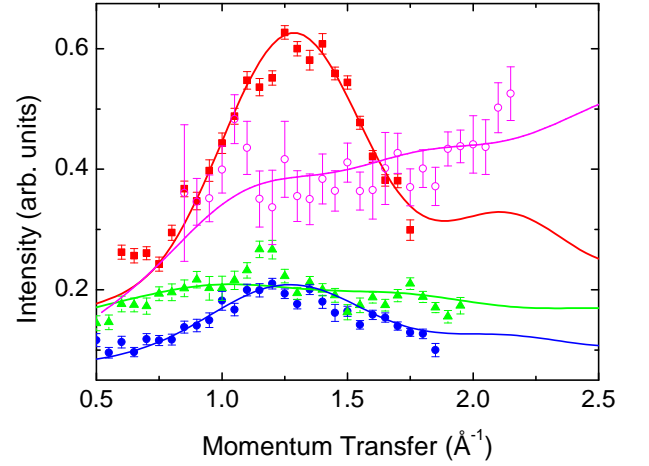


FIG. 7: Q dependence of the peaks appearing in the Cr_7Zn inelastic spectra shown in Figure 6, compared with theoretical estimates (solid lines). Triangles $|S = 3/2\rangle \rightarrow |S = 1/2\rangle$ at 0.83 meV; circles $|S = 1/2\rangle \rightarrow |S = 3/2\rangle$ at 1.38 meV; squares $|S = 3/2\rangle \rightarrow |S = 5/2\rangle$ at 1.91 meV; open circles $|S = 3/2\rangle \rightarrow |S = 5/2\rangle$ at 3.6 meV.

tensities, as shown in Figure 7 where experimental data for some of the excitations observed are compared with curves calculated with Eq. 4. It is interesting to notice that the general behavior predicted for cyclic spin clusters by Waldmann [20] is followed also in the present case where the ring symmetry is broken by the dication.

C. Cr_7Mn

Substitution of one high-spin, $s = 5/2$, Mn^{2+} ion for a Cr^{3+} in the Cr_8 ring results in an uncompensated $|S = 1\rangle$ ground state. In the presence of purely axial anisotropy, the zero-field splitting would lead to a quasi-triplet structure, with an $|S = 1, M = \pm 1\rangle$ doublet and an $|S = 1, M = 0\rangle$ singlet separated by an energy proportional to the axial crystal field parameter. As shown in Figure 8, the $\lambda = 9$ Å high-resolution spectrum recorded at $T = 2$ K shows a broad excitation that can be fitted by the superposition of two Gaussians, each with a FWHM equal to the instrumental resolution ($19\mu\text{eV}$) and centered at 0.095 and 0.11 meV, respectively. This is a clear indication of a sizeable rhombic term in the zero-field splitting Hamiltonian. By fixing the d_{Cr} parameters to the values determined by INS for the parent Cr_8 compound ($d_{\text{Cr}} = -0.03$ meV) [15], the best fit of the data is obtained for $d_{\text{Mn}} = -3\mu\text{eV}$ (a factor two hundred smaller than the Ni case) and $e_{\text{Mn}} = e_{\text{Cr}} = 0.14d_{\text{Mn}}$. If the S mixing is neglected, the ZFS parameters describing the anisotropic splitting of the $S = 1$ ground multiplet can be obtained by projecting the complete Hamiltonian onto the corresponding subspace. We obtain $H_{S=1} = D(S_z^2 - S(S+1)/3) + E(S_x^2 - S_y^2)$ with a rhombicity $E/D = 0.13$. The latter is reduced by S

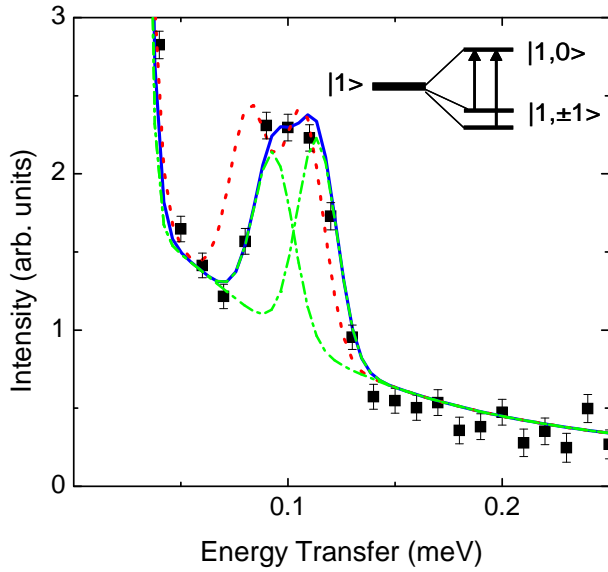


FIG. 8: Cr_7Mn high-resolution INS spectra collected with $\lambda = 9 \text{ \AA}$ at $T = 2 \text{ K}$. Two intra-multiplet transitions within the anisotropy split components of the $|S = 1\rangle$ ground state are observed. The solid line is the intensity calculated assuming both axial and in-plane anisotropy. The dash-dot lines represent the individual contributions to the broad, unresolved excitation from the transitions between the split $|S = 1, M = \pm 1\rangle$ quasi-doublet and the $|S = 1, M = 0\rangle$ singlet. The dot line gives the intensity calculated with S-mixing set to zero. The elastic peak and a quasielastic contribution have been included.

mixing to $E/D = 0.1$ (see Fig. 8).

Intermultiplet excitations measured with incident wavelength $\lambda = 4 \text{ \AA}$ are shown in Figure 9. At $T = 2 \text{ K}$ only one strong magnetic peak is observed at 1.6 meV. A second magnetic transition appears at 2.3 meV if the sample is heated at 12 K. The two peaks correspond to the transitions involving the ground state $|S = 1\rangle$ and the $|S = 2\rangle$ and $|S = 3\rangle$ multiplets with minimal energy.

Both peaks therefore correspond to excitations within the lowest rotational-like band and their energy follows the Landé rule very closely. In these conditions, only an average exchange parameter can be estimated. Assuming $J_{\text{Cr-Cr}} = J_{\text{Cr-Mn}} = 1.43 \text{ meV}$, calculations provide the spectra shown in Figure 9 by smooth lines. The agreement is satisfactory and a model with more parameters would not be justified by the data. Alternatively, by fixing $J_{\text{Cr-Cr}} = 1.46 \text{ meV}$ as in Cr_7Ni , the same results are obtained with $J_{\text{Cr-Mn}} = 1.37 \text{ meV}$. The assignment of the two transitions to the Landé-band is corroborated by the Q -dependence of their intensity, shown in Figure 10. For both peaks a pronounced oscillatory behavior is observed, whilst an almost flat Q dependence is expected for transitions to states not belonging to the rotational band.

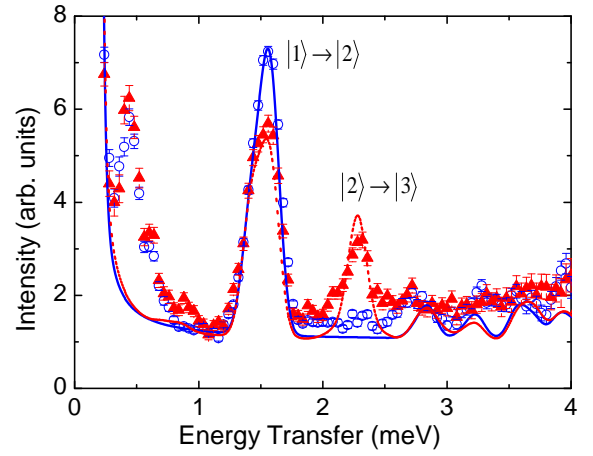


FIG. 9: Inelastic spectra at $T = 2 \text{ K}$ (circles) and $T = 12 \text{ K}$ (triangles) obtained for Cr_7Mn with an incident wavelength $\lambda = 4 \text{ \AA}$. The peak at 0.4 meV is due to spurious effects. Smooth lines are intensities calculated at 2 K (solid) and 12 K (dashed). The elastic peak and a quasielastic contribution have been included.

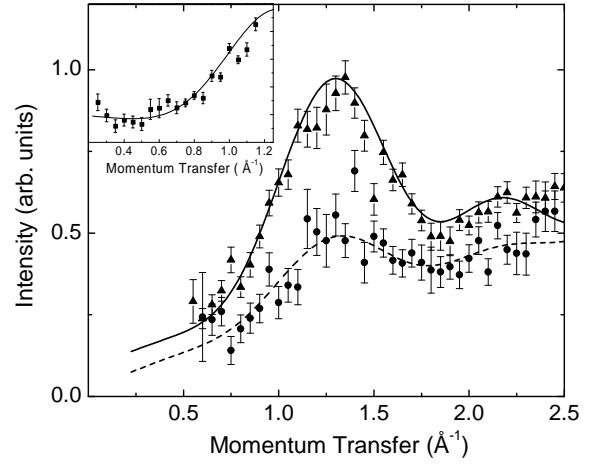


FIG. 10: Q -dependence of the peaks appearing in the Cr_7Mn inelastic spectrum at 12 K, compared with theoretical estimates: $|S = 1\rangle \rightarrow |S = 2\rangle$ at 1.6 meV (triangles and solid line); $|S = 2\rangle \rightarrow |S = 3\rangle$ at 2.3 meV (circles and dashed line). The Q -dependence of the intramultiplet transition at 0.1 meV ($T = 2 \text{ K}$) is compared with calculations in the inset.

V. DISCUSSION

The energy spectra of the heterometallic Cr_7M magnetic wheels resulting from our INS investigation are shown in Figure 11 as functions of the total spin, S . A parabolic band, formed by states with minimal energy for each S value, is easily identified. The levels belonging to this parabolic band have energies that closely follow the Landé interval rule, $E_S = \Delta_{10}[S(S+1) - S_0(S_0+1)]/[S_1(S_1+1) - S_0(S_0+1)]$, where S_0 is the spin of the ground state and Δ_{10} is the energy of the first excited level, with spin S_1 . Excitations involving adjacent

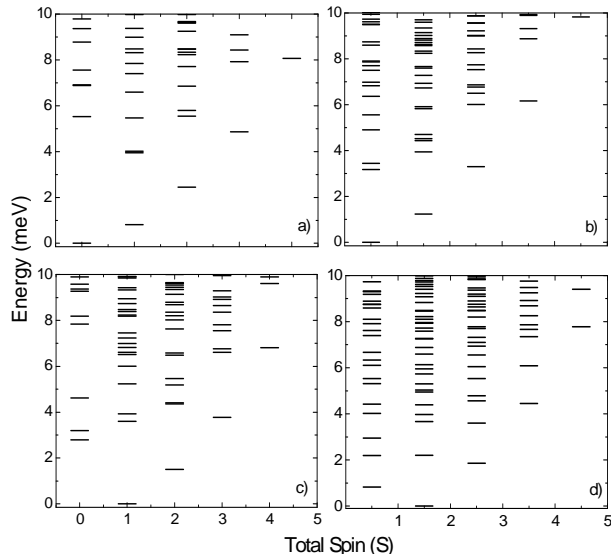


FIG. 11: Energy of the lowest spin eigenstates as a function of the total spin S calculated for Cr_7M magnetic wheels; a) $\text{M} = \text{Cr}$, b) $\text{M} = \text{Ni}$, c) $\text{M} = \text{Mn}$, d) $\text{M} = \text{Zn}$. Isotropic exchange interactions only are assumed, with parameters a) $J_{\text{Cr}-\text{Cr}} = 1.46$ meV [15], b) $J_{\text{Cr}-\text{Cr}} = 1.46$ meV and $J_{\text{Cr}-\text{Ni}} = 1.69$ meV, c) $J_{\text{Cr}-\text{Cr}} = 1.43$ meV and $J_{\text{Cr}-\text{Mn}} = 1.43$ meV, and d) $J_{\text{Cr}-\text{Cr}} = 1.43$ meV and $J_{\text{Cr}-\text{Zn}} = 0$.

levels of the parabolic band have intensities with similar Q dependencies, with an oscillatory behavior and a pronounced maximum at a Q value related to the radius of the wheel [3]. As discussed in [2, 3], these excitations are related to the combined quantum rotation of the oppositely oriented total spin on each Néel sublattice of the AF wheel [25].

Effects due to the mixing of different spin multiplets have been considered. Such effects proved to be important to correctly reproduce the energy and intensity of magnetic excitations in the neutron spectra. An interesting difference between the spin wavefunctions of the parent Cr_8 ring and those of the heterometallic derivatives concerns their symmetry. In Cr_8 the ground state and the first excited state belong to different irreducible representations of the molecule point group, whereas they have the same symmetry in the substituted wheels. This has important consequences on the system behavior in the presence of an external magnetic field. In Cr_8 the Zeeman splitting of the $|S = 1, \pm 1\rangle$ doublet leads to

a crossing with the ground state at $B = 6.9$ T with no level repulsion and a vanishingly small Schottky anomaly in the heat capacity [18]. On the other hand, according to the results of the diagonalization of the Hamiltonian Eqs. 1-2, anticrossings between the lowest lying levels are expected in the Cr_7M compounds. At the anticrossing conditions, a finite Schottky anomaly will occur, with an amplitude that depends on the angle between the applied magnetic field and the easy-axis. Moreover, the enhancement of S -mixing at the level anticrossings will produce maxima in the torque signal corresponding to oscillations of the total spin amplitude, as observed for the $\text{Mn}[3 \times 3]$ grid [8, 9].

In the investigated series, Cr_7Ni is particularly interesting. The amount of S -mixing in this ring is quite small, corresponding to about 1% admixture of $S \neq 1/2$ components in the ground state. Cr_7Ni can therefore be considered as an effective $S = 1/2$ system suitable for the implementation of the qubit [13].

VI. SUMMARY

Intra-multiplet and inter-multiplet excitations involving spin manifolds with energy smaller than 4 meV have been measured with Inelastic Neutron Scattering in polycrystalline samples of the heterometallic wheels Cr_7M ($\text{M} = \text{Ni}, \text{Mn}, \text{Zn}$). The minimum set of exchange and local crystal field parameters necessary to describe the physics of each investigated compound has been determined by comparing the experimental spectra with theoretical cross-sections. The results obtained show that chemical substitution of magnetic ions in a cyclic structure can be used to tailor the magnetic properties of the wheels, by controlling the microscopic exchange interaction. Finally, the explicit form of the general powder-averaged INS cross-section given in Ref. [20] and suitable to describe molecular nanomagnets of any symmetry has been presented.

Acknowledgments

This work was partly supported by Ministero dell'Università e della Ricerca Scientifica e Tecnologica, FIRB Project RBNE01YLKN and by EPSRC(UK). We thank the Institut Laue Langevin, Grenoble, France for access to the neutron beam facility.

-
- [1] J. Schnack and M. Luban, Phys. Rev. B **63**, 014418 (2000).
 - [2] O. Waldmann, T. Guidi, S. Carretta, C. Mondelli, and A. L. Dearden, Phys. Rev. Lett. **91**, 237202 (2003).
 - [3] O. Waldmann, Phys. Rev. B **65**, 024424 (2001).

- [4] F. Larsen, E. McInnes, H. E. Mkami, J. Overgaard, S. Piligkos, J. Rajaraman, E. Rentschler, A. Smith, G. Smith, V. Boote, et al., Angew. Chem., Int. Ed. **42**, 101 (2003).
- [5] F. Larsen, J. Overgaard, S. Parsons, E. Rentschler,

- A. Smith, G. Timco, and R. Winpenny, *Angew. Chem., Int. Ed.* **42**, 5978 (2003).
- [6] F. Meier, J. Levy, and D. Loss, *Phys. Rev. Lett.* **90**, 047901 (2003).
- [7] F. Meier, J. Levy, and D. Loss, *Phys. Rev. B* **68**, 134417 (2003).
- [8] S. Carretta, P. Santini, E. Livioti, N. Magnani, T. Guidi, R. Caciuffo, and G. Amoretti, *Eur. Phys. J. B* **36**, 169 (2003).
- [9] O. Waldmann, S. Carretta, P. Santini, R. Koch, A. G. M. Jansen, G. Amoretti, R. Caciuffo, L. Zhao, and L. K. Thompson, *Phys. Rev. Lett.* **92**, 096403 (2004).
- [10] S. Carretta, E. Livioti, N. Magnani, P. Santini, and G. Amoretti, *Phys. Rev. Lett.* **92**, 207205 (2004).
- [11] J. van Slageren, R. Sessoli, D. Gatteschi, A. Smith, M. Helliwell, R. Winpenny, A. Cornia, A.-L. Barra, A. Jansen, E. Rentschler, et al., *Chem. Eur. J.* **8**, 277 (2002).
- [12] M. Affronte, A. Ghirri, S. Carretta, G. Amoretti, S. Piligkos, G. Timco, and R. Winpenny, *Appl. Phys. Lett.* **84**, 3468 (2004).
- [13] F. Troiani, A. Ghirri, M. Affronte, S. Carretta, P. Santini, G. Amoretti, S. Piligkos, G. Timco, and R. Winpenny, *arXiv:cond-mat/0405507* (2004).
- [14] R. Caciuffo, G. Amoretti, A. Murani, R. Sessoli, A. Caneschi, and D. Gatteschi, *Phys. Rev. Lett.* **81**, 4744 (1998).
- [15] S. Carretta, J. van Slageren, T. Guidi, E. Livioti, C. Mondelli, D. Rovai, A. Cornia, A. Dearden, M. Affronte, C. Frost, et al., *Phys. Rev. B* **67**, 094405 (2003).
- [16] T. Guidi, S. Carretta, P. Santini, E. Livioti, N. Magnani, C. Mondelli, O. Waldmann, L. K. Thompson, L. Zhao, C. D. Frost, et al., *Phys. Rev. B* **69**, 104432 (2004).
- [17] S. Carretta, P. Santini, G. Amoretti, T. Guidi, R. Caciuffo, A. Candini, A. Cornia, D. Gatteschi, M. Plazenet, and J. Stride, *Phys. Rev. B* **70**, 0 (2004).
- [18] M. Affronte, T. Guidi, R. Caciuffo, S. Carretta, G. Amoretti, J. Hinderer, I. Sheikin, A. Jansen, A. Smith, R. Winpenny, et al., *Phys. Rev. B* **68**, 104403 (2003).
- [19] J. J. Borrás-Almenar, J. M. Clemente-Juan, E. Coronado, and B. S. Tsukerblat, *Inorg. Chem.* **38**, 6081 (1999).
- [20] O. Waldmann, *Phys. Rev. B* **68**, 174406 (2003).
- [21] B. S. Furniss, A. J. Hannaford, P. W. G. Smith, and A. R. Tatchell, *Vogel's Textbook of Practical Organic Chemistry, 5th ed* (Longman Scientific & Technical, New York, 1989).
- [22] W. Marshall and S. Lovesey, *Theory of Thermal Neutron Scattering* (Clarendon Press, Oxford, 1971).
- [23] E. Livioti, S. Carretta, and G. Amoretti, *J. Chem. Phys.* **117**, 3361 (2002).
- [24] This is the value needed to reproduce the observed anisotropy splitting of the $|S = 3/2\rangle$ manifold by assuming $d_{Ni} = d_{Cr}$.
- [25] P. Anderson, *Phys. Rev.* **86**, 694 (1952).

